Calibrated MFM Measurement of Current-carrying Lines

R. Yongsunthon, J. McCoy, E. D. Williams

Department of Physics, University of Maryland

College Park, MD 20742-4011 U.S.A

Abstract

An experimental configuration for evaluating the MFM instrument response for known structures, such as that around current-carrying lines containing defects of simple geometry, has been developed. The configuration includes mechanisms for nulling electrostatic potential and providing an in-situ reference structure adjacent to the test structure. The reference structure is used to normalize the signal magnitude from the test structure. The instrumental response function was determined iteratively by comparing the forward convolution of the calculated magnetic response with the measured signal from a 10μm wide, 110nm thick Cr/Au-on-SiO_2 structure. This response function was then used in a MEM deconvolution of signals from a 10μm wide line containing a 3μm×40μm slot. Preliminary results show that meaningful relative quantification of the MFM signal amplitude can be achieved to within 10%, absolute current variations can be detected to at least 10%, and spatial variation in current can be resolved to at least 1μm.

Introduction

The theory of electromigration, which describes the motion of atoms under the influence of applied electric fields, is of great interest for both the fundamental physics and potential technological applications involved [1,2,3]. The study of electromigration in metals requires correlation of current densities with the evolution of defects in current-carrying lines. In principle, magnetic force microscopy (MFM) [4] is an appropriate probing tool that allows direct imaging of the curvature of the magnetic fields around defect structures and thus deduce the underlying current densities. Previous use of MFM has concentrated upon determining magnetic polarity, and there has been little evaluation of MFM capability to make meaningful quantification. Although several research groups have attempted to calibrate the magnetic probes [5,6,7,8,9], few calibrations [8] are appropriate for electromigration studies, and none have incorporated an in-situ reference for evaluating the tip response. We have developed an experimental configuration for evaluating the MFM instrument response for known current-carrying structures. Our configuration includes mechanisms for nulling electrostatic potential and providing an in-situ reference structure adjacent to the test structure.

Experimental Technique

Experiments were performed using Scanning Probe Microscopy (SPM), operated in Atomic Force Microscopy (AFM) tapping (intermittent non-contact) mode.

Evaluation of current densities was performed using Magnetic Force Microscopy (MFM) imaging.

MFM phase response techniques involve extracting information from the phase response of the oscillating cantilever as its tip passes over the sample. The cantilever is initially driven at resonance away from the sample, such that the phase between the driving force and the cantilever response is 90^{o}. The frequency of the driving force is kept constant as the tip approaches the sample surface. Near the surface, the interaction forces change the effective spring constant of the cantilever, changing its natural resonance frequency and thus forcing the phase to change, as follows:

$$\Delta j = -\left(\frac{\boldsymbol{Q}}{\mathbf{k}}\right)_{\mathbf{can}} \frac{\partial \boldsymbol{F}_{\mathbf{int}}}{\partial \boldsymbol{z}} \qquad (1)$$

where the quality factor, *Q*, and the spring constant, *k*, are constants dependent upon the individual tip-cantilever system used; F_{int} is the interaction force and *z* is the distance perpendicular to the sample surface.

Standard Digital Instruments MESP tips, magnetized perpendicular to the sample surface, are used. The following expression, using the interaction force from a magnetic dipole probe [10], for the change in phase allows us to extract information about changes in the current density from the measured MFM response:

$$\Delta j = -\left(\frac{\boldsymbol{Q}}{\mathbf{k}}\right)_{\mathbf{can}} \mathbf{m}_z \frac{\partial^2 \boldsymbol{B}_z}{\partial \boldsymbol{z}^2} \qquad (2)$$

To ensure that the MFM phase signal accurately represents only the magnetic force interaction, any topographical and/or electrostatic interaction must be eliminated. Phase data is thus taken at a significant lift height above the sample surface, to eliminate effects due to topography. There are two common lift modes, available as standard Digital Instruments software: Interleave Lift Mode and Linear Mode [11]. Linear Mode eliminates phase artifacts due to tip-sample collision and is our preferred lift mode [12]. Elimination of electrostatic interaction is discussed below.

To avoid the difficulties involved in determining absolute tip calibrations [5,6,7,8,9], we have developed quantification relative to the signal from a known structure, shown in Fig. 1. The sample incorporates three current-carrying lines: the left-most line is center-tapped to a tip connection and leads to a null-current line segment, the center line contains a simple defect, and the right-most line is a defect-free reference line, to be used as a basis for comparison. The tap to the tip eliminates electrostatic interactions between the tip and sample. If the tap fails, the potential between the tip and sample can be balanced, using an external voltage divider. The null-current line is imaged to insure the absence of signal from non-magnetic interaction forces. To do the calibration, the scan range is set-up to include both the defect and reference lines. The MFM signal amplitude from the reference line is well-understood and can be used to normalize the signal magnitude from the line containing the defect. The signal from the defect lines can thus be quantitatively interpreted without ambiguities that would otherwise arise due to tip demagnetization, specific tip engagement, etc.

We use a Digital Instruments Multimode AFM, where the optical head is equipped with a special low-noise laser [13]. If the standard laser diode is used, the phase signal may be dominated by laser noise. Images taken with the low-noise laser were more susceptible to laser interference patterns, but such patterns can be removed by Fast Fourier Transformation (FFT), if necessary.

The sample layout of Fig. 1 was also designed to be compatible with our Digital Instruments Multimode AFM platform and to allow for external electrical connections. The patterns are Cr/Au lines, 10μm wide and 110nm thick, on SiO_2, fabricated by liftoff.

Magnetic Field Calculations

To assess the measurement sensitivity for detection of current density variations around electromigration-induced voids, we must calculate the magnetic fields around a known structure and predict the MFM phase response expected from a typical experimental setup. Comparison of such calculations with the measured MFM signal will help us determine an instrumental response.

For simple systems where the current flows along lengths which are long compared to characteristic tip dimensions, the conductor can be treated as a bundle of infinitely long wires. The MFM tips used typically have radii of curvature of 500nm or less, and the current-carrying conductors are generally several hundred microns in length. We may therefore solve for the magnetic field around the conductor by integrating the magnetic field contributions of infinitesimally thin, infinitely long wires over the cross sectional area of the conductor [14]. An example of such a calculation, shown in Fig. 2a, is the ideal MFM phase response for a 50μm scan across the conductor width, assuming a dimensionless, delta-function tip with perfect vertical magnetization. Although the ideal signal is composed of sharp spikes near line edges, the measured signal will also depend upon tip dimensions and will thus be a broader convolution of the ideal signal and the tip-dependent instrumental response function, which will ultimately be determined experimentally.

The effect of real voids on nearby currents and fields is not easily integrable and must be numerically calculated. In the future, we will run numerical calculations, using methods such as the relaxation method, to calculate the effect of realistic voids.

Deconvolution

Given the finite dimensions of our probe, the measured signal is actually a weighted average over a region on the order of the tip size. This effect leads to deceptive signal magnitudes when measuring closely spaced signals of opposite polarity and can be removed by deconvolving the instrumental response. We iteratively determine the instrumental response by comparing the measured MFM signal from a reference structure with the forward convolution of an estimated response with the calculated MFM signal. This preliminary estimated instrumental response (see Fig. 3) is used with the Maximum Entropy Method [15,16] (MEM) for deconvolution of signal from more complicated structures.

Experimental Results

MFM images from a sample fabricated with a 3μm×40μm slot are shown in Figs. 4 and 5. The height images show ear-like structures, which are artifacts of liftoff fabrication, at the line edges. In Fig. 5, we take repeated scans to improve statistics and change current directions to confirm the expected reversal of signal polarity. An average of repeated lines scans across the structure is shown in Fig. 2b. The null-current line (see Fig. 1, left line segment, for reference) shows no phase response, indicating that we are detecting phase shifts solely due to magnetic interactions.

Below (or above) the slot, the slotted line is identical in geometric form to the reference line. All other factors being equivalent, their respective MFM signals differ in magnitude, solely because they carry different currents. We can thus deduce the relative currents in the two lines by comparing the magnitudes of their MFM signals. The result obtained, $I_{slot}=0.85I_{ref}$, is consistent with expectations from considerations of the change in line resistance due to the addition of the slot.

Since the slot is much longer than the tip dimensions, the magnetic field for this sample can be calculated (see Fig. 2a), assuming that the slot is infinitely long. Given a current of I_0 in the reference line and $0.85I_0$ in the slotted line, the magnitudes of the MFM signals would relate as $MFM_{slot} = 1.24\ MFM_{ref}$, if measured with an ideal dimensionless tip. To account for finite tip dimensions, we perform a forward convolution of our preliminary estimated tip profile (see Fig. 3) with the calculated ideal MFM signal of Fig. 2a. The peaks of this forward convolution, shown in Fig. 2c, are broader than the ideal-tip peaks of Fig. 2a and match the measured response, shown in Fig. 2b, remarkably well. A straight average of the raw data yields $MFM_{slot} = 1.12\ MFM_{ref}$, 10% lower than the value in the ideal-tip calculation (see Fig. 2a) and 3% lower than the result of the forward convolution (see Fig. 2c). A deconvolution of the averaged raw data (see Fig. 2d), using our preliminary estimated tip profile (see Fig. 3), yields $MFM_{slot} = 1.34\ MFM_{ref}$, 8% higher than expected from ideal-tip calculations. The quality of the deconvolution is expected to improve as the tip profile and MEM algorithm are improved.

Conclusion

By comparing MFM phase measurements with theoretical calculations of MFM response around simple line structures, we have estimated a useful instrumental response for quantitative evaluation of MFM data.

Preliminary results show that meaningful relative quantification of the signal can be achieved to within 10%, absolute current variations can be detected to at least 10%, and spatial variation in current can be resolved to at least 1μm.

Studies of smaller defects and use of higher resolution magnetic tips will extend the limits of MFM detection capability and will be necessary for future studies of electromigration-induced void behavior.

Acknowledgements

This work was supported by the University of Maryland NSF-MRSEC under grant #DMR-00-80008.

References:

1. E. Kinsbron, Appl. Phys. Lett. 36, 968 (1980)

2. Y.-C. Joo, C. V. Thompson, S. P. Baker, E. Arzt, J. Appl. Phys. 85, 2108 (1999)

3. R. J. Gleixner, W. D. Nix, J. Appl. Phys. 86, 1932 (1999)

4. Roger Proksch, E. Dan Dahlberg, Rev. Sci. Instrum. 64, 912 (1993)

5. T. Goddenhenrich, H. Lemke, M. Muck, U. Hartmann and C. Heiden, Appl. Phys. Lett. 57, 2612 (1990)

6. K. Babcock, V. Elings, J. Shi, D.D. Awshalom and M. Dugas, Appl. Phys. Lett. 69, 705 (1996)

7. R. Proksch, G.D. Skidmore, E.D. Dahlberg, S. Foss, J.J. Schmidt, C. Merton, B. Walsh and M. Dugas, Appl. Phys. Lett. 69, 2599 (1996)
8. R.D. Gomez, A.O. Pak, A.J. Anderson, E.R. Burke, A.J. Leyendecker, and I.D. Mayergoyz, J. Applied Physics, volume 83, issue 11, 6226 (1998)
9. P. J. A. van Schendel, H. J. Hug, B. Stiefel, S. Martin, and H.-J. Güntherodt, J. Appl. Phys. 88, 435 (2000)
10. P. Grutter, H.J. Mamin, and D. Rugar, in Scanning Tunneling Microscopy Vol.II edited by Wiesendanger and H.K.Guntherodt (Springer, Berlin, 1992), p. 151
11. Digital Instruments technical support, private communication
12. R. Yongsunthon, J. McCoy, E.D. Williams, 2000 ULSI Conference Proceedings, NIST, Gaithersburg, Maryland, June 2000, in press
13. Digital Instruments part# 226-000-004, available by special request from technical support
14. E.M. Purcell, Electricity and Magnetism, McGraw Hill College Div (1984)
15. E.T. Jaynes, Physical Review, vol.106, no.4, pp.620-630 (1957)
16. J. Skilling and S.F. Gull, reprinted f. "Maximum-Entropy and Bayesian Methods in Inverse Problems", C. Ray Smith and W.T. Grandy Jr. (eds.), D. Reidel Publishing, pp.83-132 (1985)

Figure Captions:

Figure 1. The sample incorporates three current-carrying lines: the left-most line is center-tapped to a tip connection and leads to a null-current line segment (to detect any unwanted electrostatic force interaction), the center line contains

a simple defect, and the right-most line is a defect-free reference line, to be used as a basis for comparison.

Figure 2. The conductor cross section is shown as a dotted line, for positional reference.

a) The thick line is the calculated ideal MFM phase response for a 50μm scan across the conductor (center and right lines in Fig. 1) width with the tip lifted 350nm above the sample surface. Typical tip parameters used: $(Q/k)_{cantilever}$ = 2300 degN/m; $m_z = 8.2\times10\text{-}15\ Am^2$.

b) The thick line is a straight average of the raw MFM data. Part of the null-current line lies between 0 and 5μm. The slotted line lies between 10 and 25 μm and carries 18mA. The reference line lies between 30 and 45μm and carries 21mA.

c) The forward convolution of the calculated ideal MFM phase response, shown in Fig. 2a, with our estimated tip profile, shown in Fig. 3.

d) The thick line is an MEM deconvolution of an average of the raw MFM data. Part of the null-current line lies between 0 and 5μm. The slotted line lies between 10 and 25 μm and carries 18mA. The reference line lies between 30 and 45μm and carries 21mA.

Figure 3. Estimated tip profile found by comparing the forward convolution of the calculated magnetic response with the measured signal from a 10μm wide, 110nm thick Cr/Au on SiO_2 structure.

Figure 4. 40μm×40μm image of slotted and reference lines, carrying 22mA and 26mA currents, respectively. a) AFM topography of sample with slotted test structure. b) Corresponding MFM phase with 350nm linear lift height.

Figure 5. 50 μm-wide repeated scans at the center of the slot, with occasional changes in direction of current. The left-most line segment carries is the null-current segment, the center line is the slotted line, carrying 18mA, and the right-most line is the reference line, carrying 21mA. a) AFM topography. b) Corresponding MFM phase, given a linear lift of 250nm. Note the absence of the null-current line in the MFM signal, implying that only magnetic interaction is being detected. Also note that the contrast of the MFM signal changes polarity as the current is reversed.

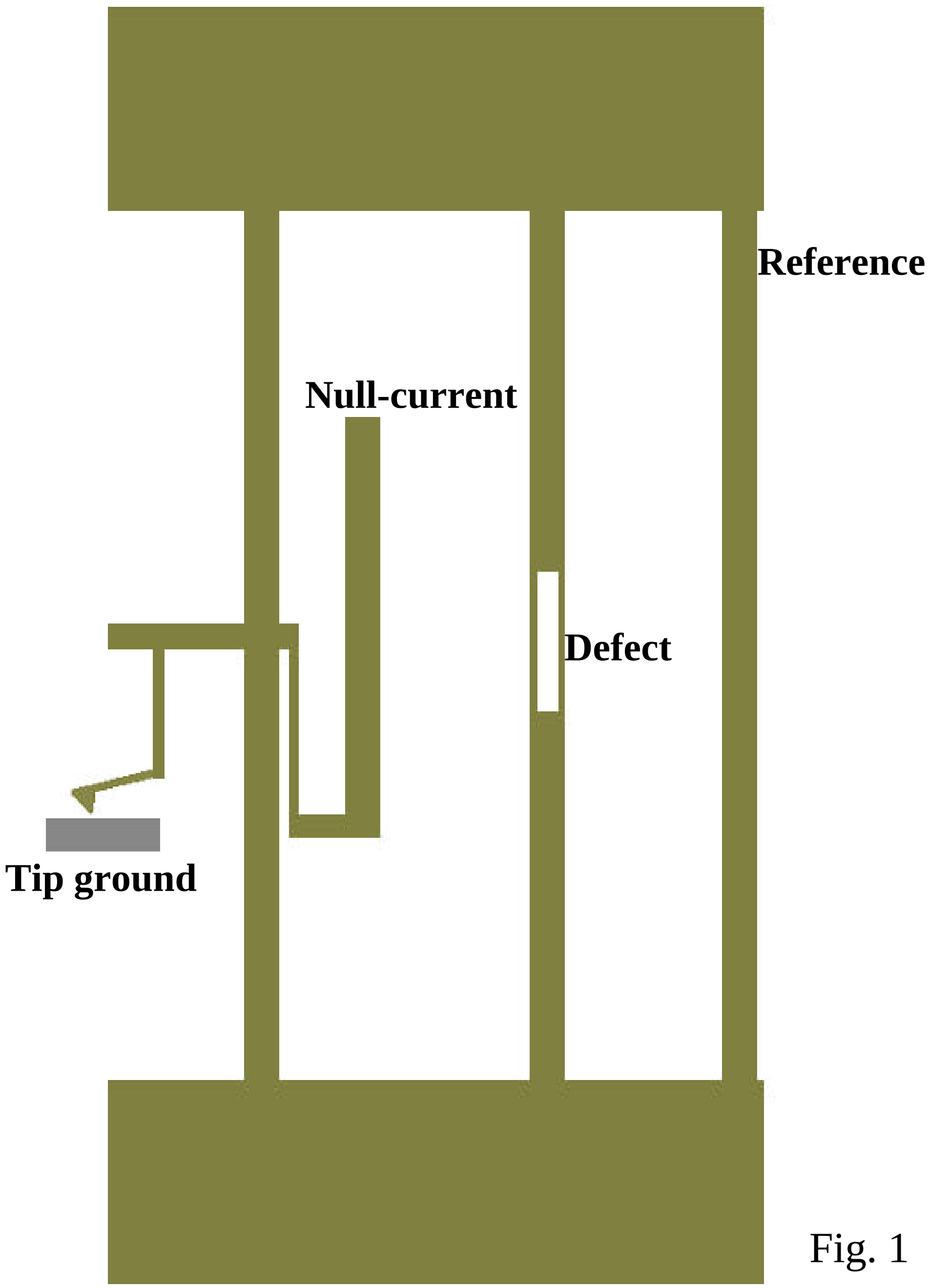

Fig. 1

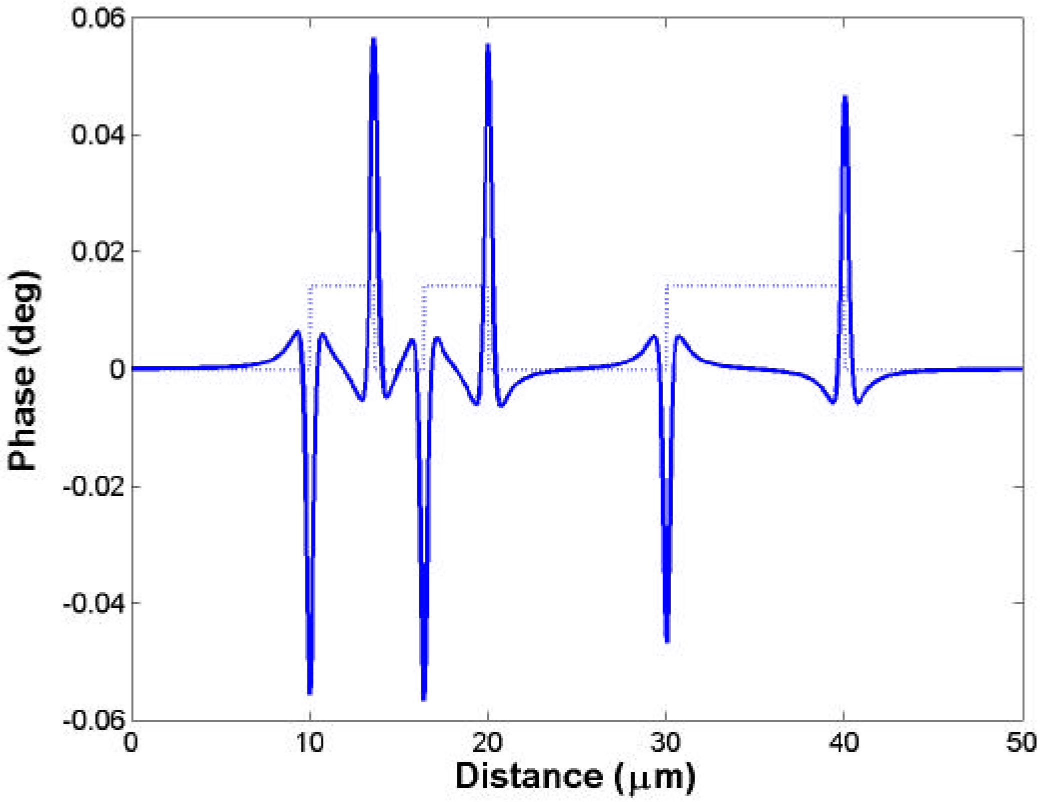

Fig. 2a

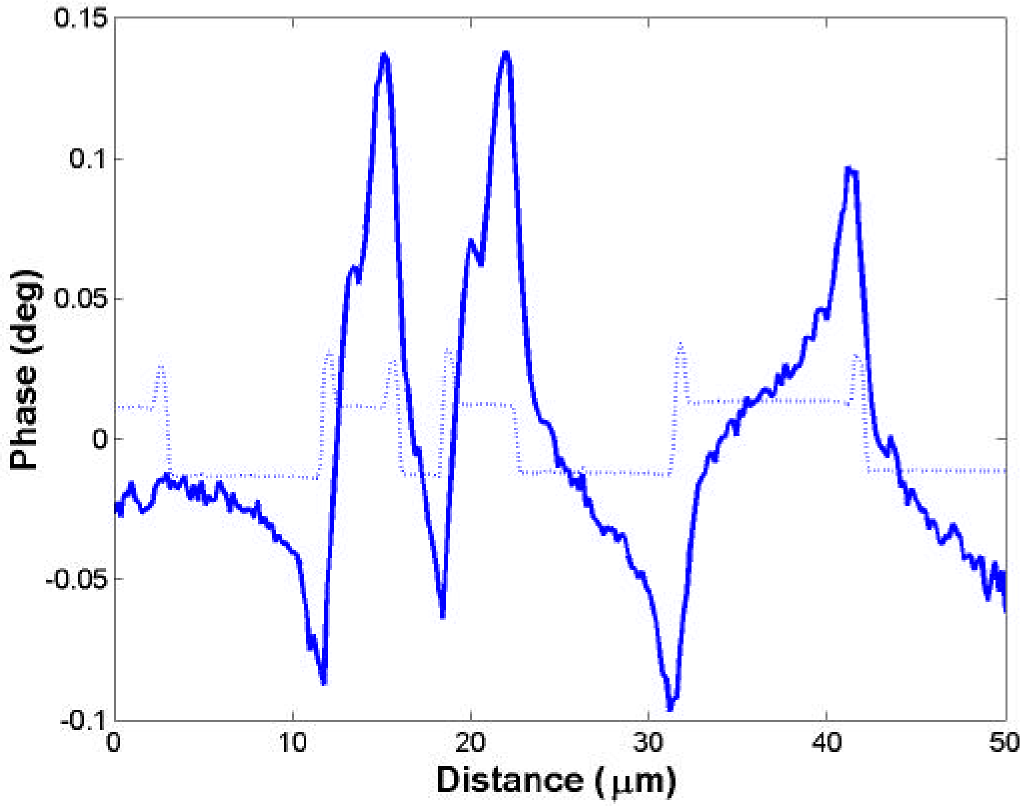

Fig. 2b

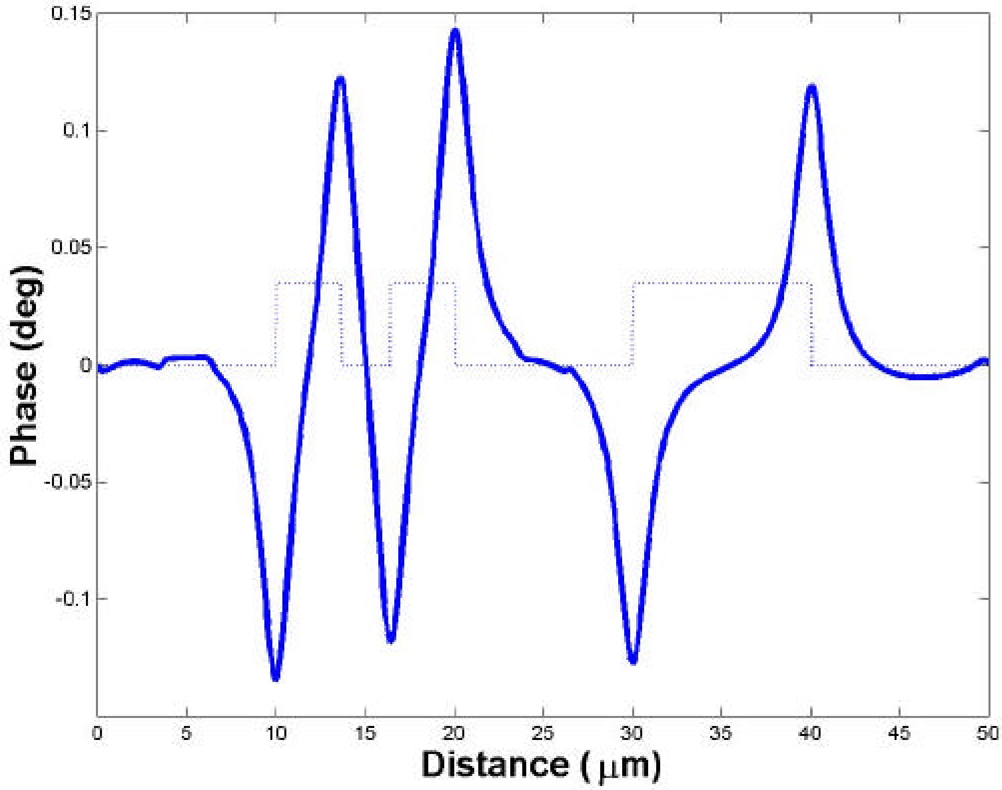
0.15
0.1
0.05
0
-0.05
-0.1
Phase (deg)
0
5
10
15
20
25
30
35
40
45
50
Distance (μm)

Fig. 2c

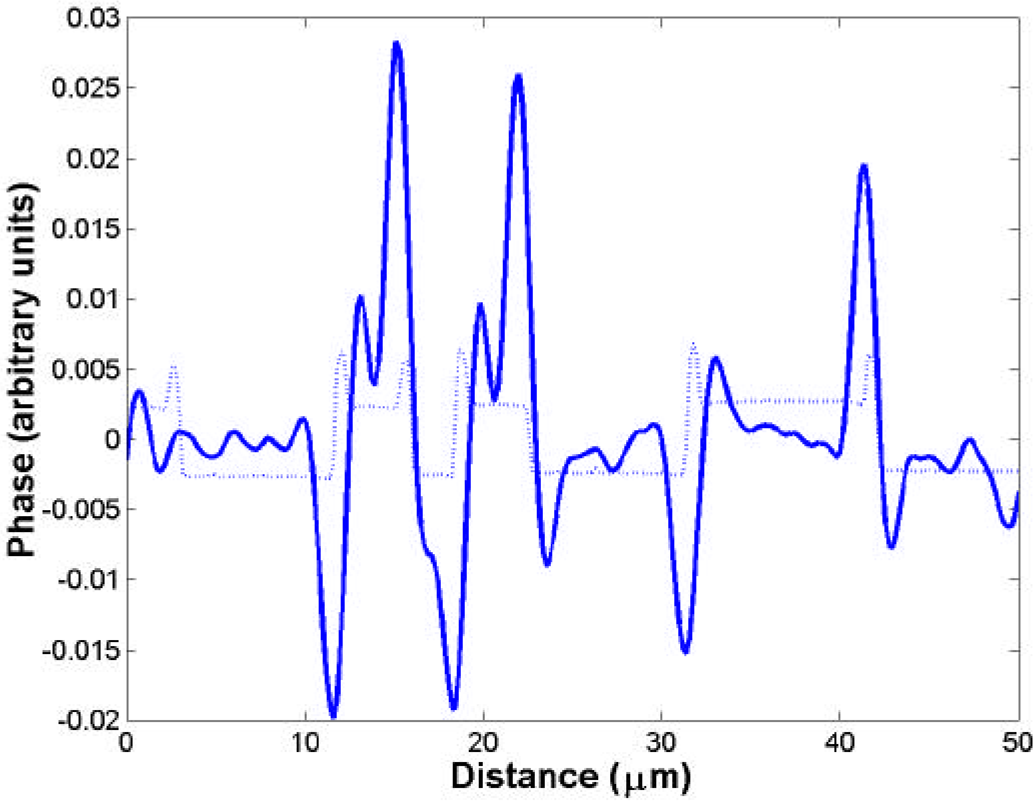

0.03
0.025
0.02
0.015
0.01
0.005
0
-0.005
-0.01
-0.015
-0.02
Phase (arbitrary units)
0
10
20
30
40
50
Distance (μm)

Fig. 2d

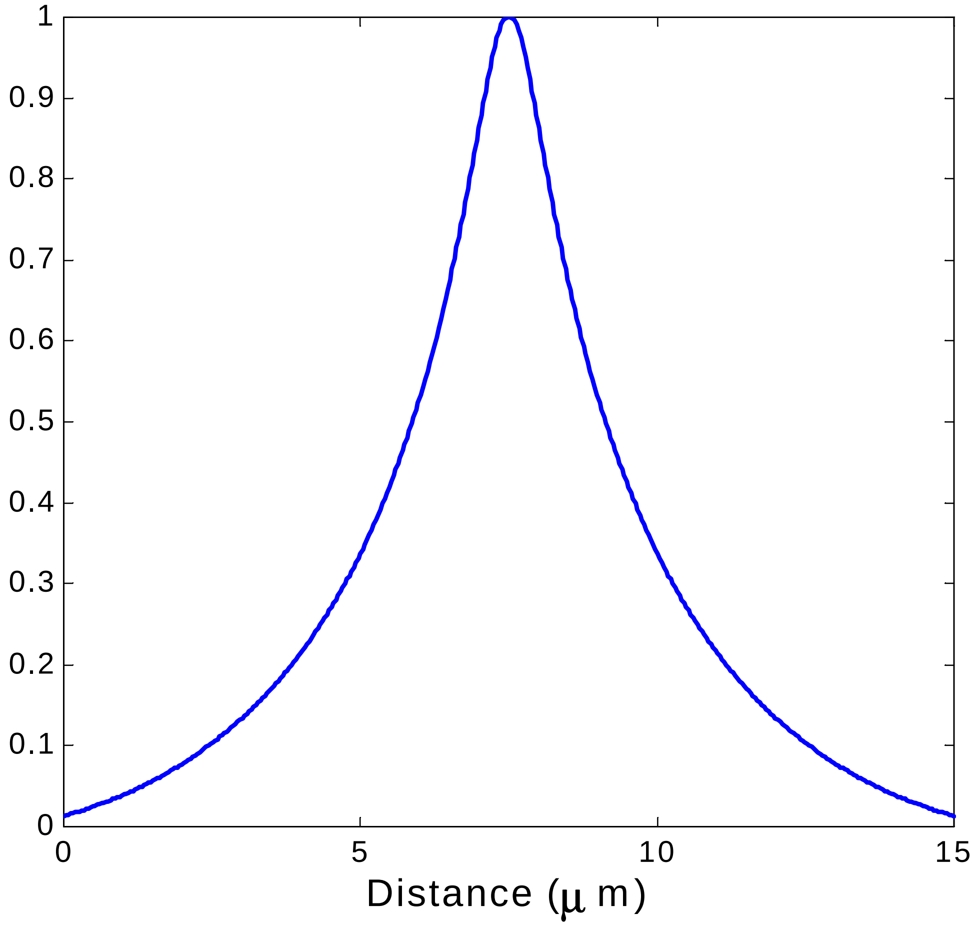

Fig. 3

Topography **MFM Phase with ~25mA per line**

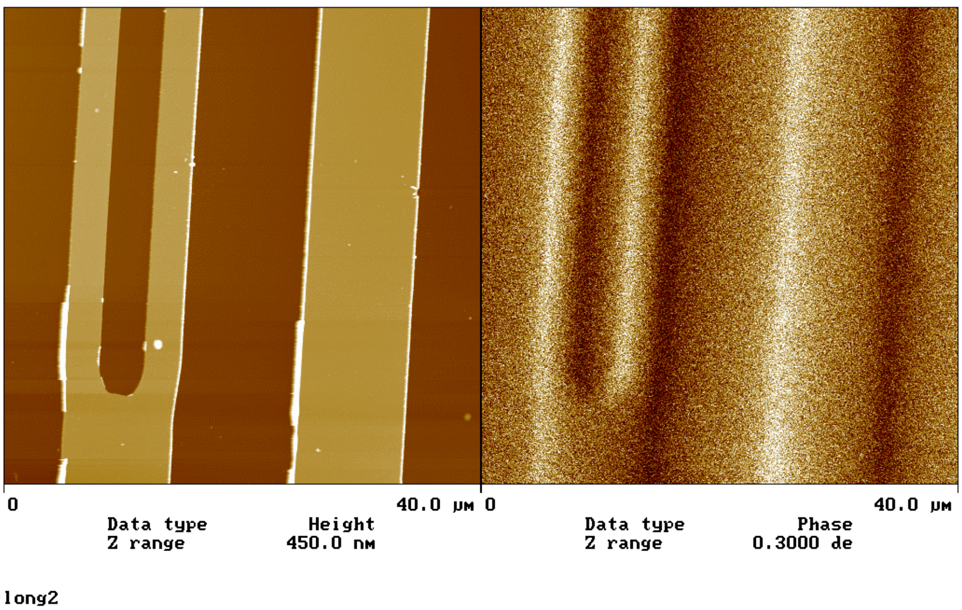

Fig. 4

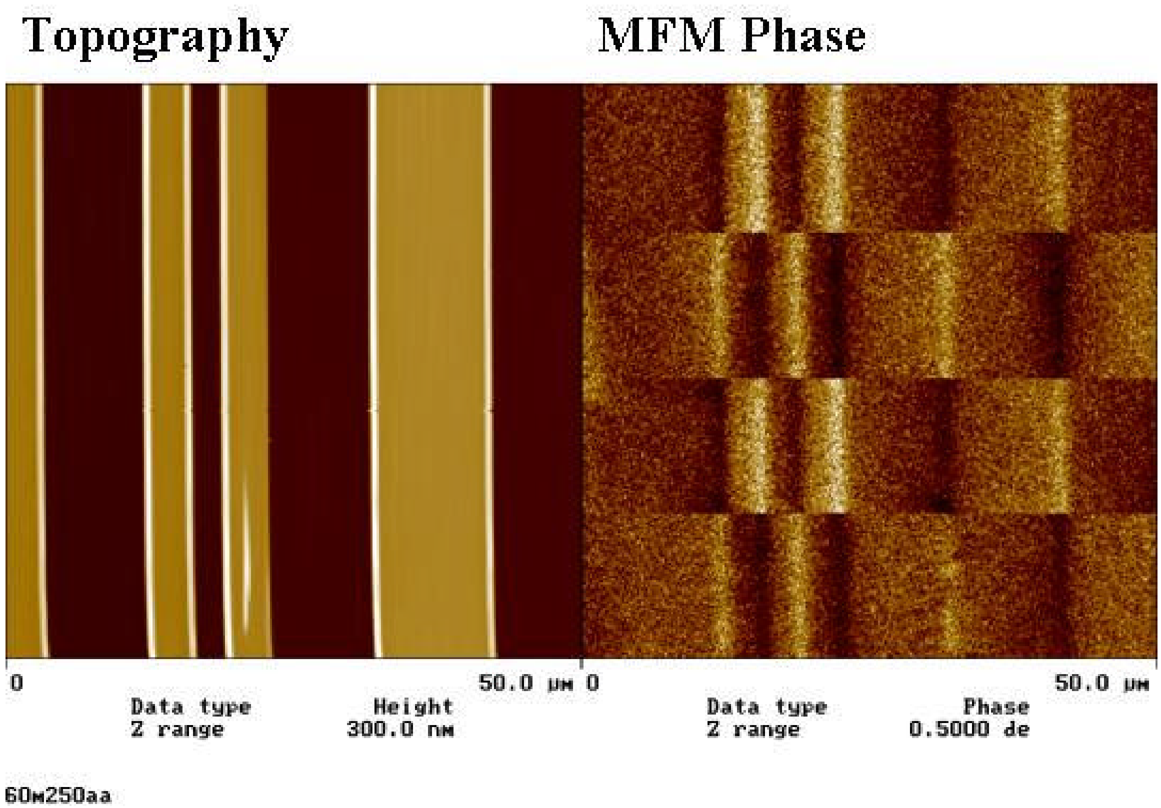
Topography
MFM Phase
0
50.0 µm
0
50.0 µm
Data type
Height
Z range
300.0 nm
Data type
Phase
Z range
0.5000 de
60m250aa

Fig. 5